

Diagnosics for particulate vaporization and interactions with surfaces

Armelle Vardelle, Michel Vardelle, P.Fauchais

Laboratoire Céramiques Nouvelles URA CNRS 320
University of Limoges, 123 Rue A.Thomas, Limoges, 87000 France

Abstract - Plasma spraying deposition is a fast and powerful technique to produce protective coatings on various substrates. To understand the relationship between the spraying process and the quality of the coatings, there is a need to study plasma/ particulates and particulates/substrate interactions.

The first part of this paper refers to the main techniques used at the present time to investigate the impact and cooling of the molten particulate stream on the substrate.

In the second part, experiments conducted to study particulate vaporization into the plasma jet are reported.

INTRODUCTION

Thermal spraying is a group of processes in which finely divided metallic or non metallic materials are deposited in a molten or semi-molten condition on a prepared substrate to form a spray deposit (ref 1,2). Particulates strike the surface, flatten and form thin platelets (splats) that conform and adhere first to the irregularities of the prepared surface and then to each other.

The factors controlling the microstructure and thus the thermo-mechanical properties of the resulting coating are clearly the particulate velocity, size and temperature (viscosity) upon impact and the conditions under which the particulates spread and solidify on the substrate. The interactions between the plasma jet and the particulates and those between the particulates and the substrate are highly related. A basic understanding of plasma coating formation requires the knowledge of the particulates thermal history both in the plasma flow and during their flattening and cooling process.

If the mechanisms of particulate heating and acceleration within the plasma jet have been studied extensively (ref 3,4,5), the particulates-substrate interactions have received less attention. This paper will present the main techniques used at the present time to investigate splat formation. These are the examination of individual splats, the monitoring of acoustic emission during spraying and the measurement of the time-temperature evolution of the impinging particulates.

Studies of the impact of droplets onto hot substrates in spray cooling process (ref 6) have shown that a film of vapour between the drop and the substrate prevents contact and may cause the drops rebound. Under plasma spraying conditions, the vaporization of particulates is expected to be high, as pointed out both by computations (ref 7,8) and experiments (ref 9). Thus this paper will be ended by a discussion of the experiments conducted to investigate the particulate vaporization into the plasma jet.

PARTICULATE SUBSTRATE INTERACTIONS DURING PLASMA SPRAYING

It is well established (ref 10) that a plasma sprayed coating is built by discrete particulates which have followed different trajectories and thus undergone various thermal histories in the plasma jet. According to the classical spraying conditions (about 2 kg/h of injected powder) the mean time elapsed between the flattening of two particulates at the same location is in the order of 1 ms while the mean time for a particulate to solidify is in the range of ten microseconds. Thus a particulate flattens either on the substrate or on already solidified particulates. During this flattening process, the impacted particulate experiences two simultaneous phenomena (ref 11): solidification and radial spread of liquid flow.

The modelling of these phenomena is rather complex and has been developed at the present time only for simplified situations. The first studies of Madjeski (ref 11) took up again by Mc Pherson (ref 13) and Hamatani (ref 14) show clearly the importance of the particulate temperature T_p upon impact compared to its velocity. When T_p is close to or higher than the melting temperature T_m , the particulate viscosity is drastically reduced and the ratio of the lamella diameter (D) to that (d) of the initial particulate increased (in a range 3 to 7). That is why good coatings are obtained with molten or partially molten particulates upon impact.

The recent work of Houben (ref 10) has tried to precise the conditions for molybdenum flattening particulates for which the temperature can be assumed to be uniform upon impact. Starting from the observation of different splats collected on glass slides, Houben has shown that it is necessary to account for a shock wave propagation in the flattening particulate, shock wave modifying the liquid

flow of the spreading droplet. His calculations indicate for a given particulate temperature T ($T > T_m$) the existence of a critical radius r_c over which a material flow develops parallel to the substrate limiting the contact between the lamella and the substrate ("flower" type lamella). Below r_c the central contact is much better ("pancake" type with distinct radial strings) with microcracks to relax the stresses resulting from the fast cooling. For temperatures below T_m the particulate is moderately spread (pancake type with no microcracks). Similar results for the contacts between the lamellae were obtained for alumina particulates by Mc Pherson (ref 13) who has shown that such contacts represent sometimes less than 10% of the lamella surface. These contacts of course control the thermophysical properties of the coatings as demonstrated by Pawlowski et al (ref 15) when annealing zirconia coatings. The phenomena are more complex when considering ceramic particulates which impact with high temperature gradients, with sometimes the central part of the particulate completely unmolten and surrounded by a molten shell, especially for porous particulates. In this case the flattening is different with the possibility for the central core to rebound on the substrate.

Due to the interactions of the phenomena involved during particulate impact, a general model for particulate flattening and solidification is difficult to establish (a detailed review of these phenomena is given by Apelian and his co-workers in (ref 16) and (ref 11)). And experimental investigations of thermal and mechanical exchange between the impinging particulates and the substrate would help to validate the assumptions of such models.

1. Particulate collection on a substrate

One of the simplest techniques used to gain information about particulate solidification is the collection of some sprayed particulates on a translated or rotated substrate (usually a glass slide) crossing the flow. The collected splats are generally observed by scanning electron microscopy or optical microscopy. Their thickness is determined from a cross section perpendicular to the substrate (mostly for metallic particulates) or using a high precision tactile profilometer.

Such experiments performed for different arc current, plasma gas flowrate and nature allow to monitor the molten state of the particulates, their microstructure after impact and their degree of flattening deformation (D/d), possibly in terms of distance from the powder injection port or/and the plasma jet centerline (where D and d are the diameters respectively of the splat and the particulate).

Many micrographs of single particulates plasma sprayed on substrates have been published (ref 17,18,19) and these micrographs show various particulates spread morphologies between a completely circular disc to exploded particulates spread into smaller particulates as illustrated schematically in fig 1 after Kudinov et al (ref 20). The microstructure of impacting droplets may differ greatly according to the nature of the sprayed material and substrate, the substrate roughness, the working conditions of the plasma process. For particulates from the same batch and sprayed in the same conditions, the microstructure depends also on their size, velocity and temperature upon impact, so that investigations from these micrographs are tedious and comprehensive studies are scarce.

For example, Houben (ref 10) has investigated the relationship between the velocity and heat content of metallic particulates (molybdenum, stainless steel, aluminium) and the morphologies of the resulting

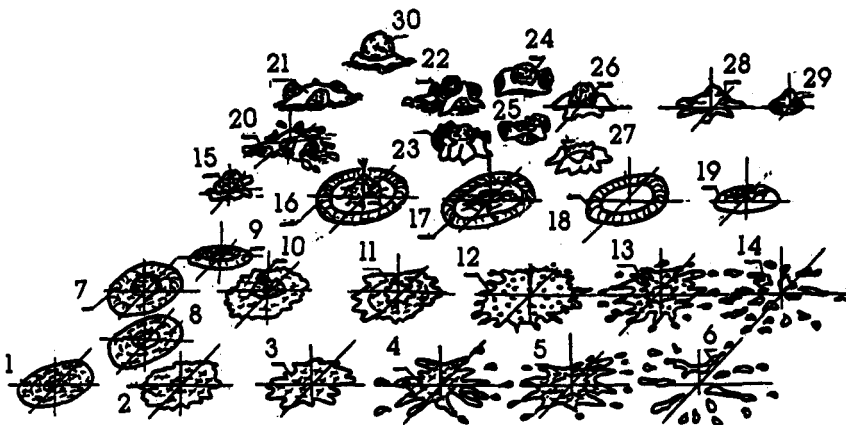


Figure 1:

Schematic representation of particulate impacts on a substrate after Kudinov et al (ref 20).

1->4 : completely melted; 7->11 : completely melted with gas fitted cavity; 12->14 : overheated, evaporating; 15->19 : with molten shell and solid nucleus; 20, 21, 30 : with solidified outshell and molten nucleus; 22->27 : with solidified outshell, melted interlayer and solid nucleus; 28, 29 : solid highly accelerated particulates

splats. The particulates velocity is estimated using a photographic method and their heat content from the temperature rise of a steel strip placed in the centerline of the spray flow. The main concluding remarks of this work are that the formation of a "flower" type splat is connected with a high velocity or heat content of the impinging droplets and is characterized by a chaplet corona, an impact crater and friction welds whereas the formation of a "pancake" type splat is connected with a moderate velocity and heat content of liquid particulates and leads to diffusion bonding or partial friction welds. The main morphologies of spread metallic particulates on steel are given in fig 2. These results on the velocity effect at impact are confirmed by those obtained by Kharlamov et al (ref 18).

The importance of the impact velocity is also underlined by some recent results presented by Boulos et al (ref 21). When spraying with an Ar-H₂ R.F. plasma, they show that well molten alumina particulates (T_p > 2500 K) (d = 21±5 μm) impacting with velocities below 50 m/s exhibit the type 2 morphology described in fig 2. The ratio D/d is between 2 and 4. With DC plasma jets (Ar-He) hydroxylapatite splats have morphologies of the type 3 or 4 and ratios D/d are between 5.7 and 9.1 (ref 19).

Hamatani and Yoshida (ref 14) have studied the influence of the plasma spraying process (radio-frequency plasma spraying: RFPS and hybrid plasma spraying: HYPS) as well as the influence of the substrate position (L) on the degree of flattening deformation of zirconia particulates sprayed on steel substrate. The main results are given in fig 3.

They show that the dependence on L is less in the case of HYPS than that of RFPS, and that the degree of particle deformation is higher with hybrid plasma spraying. This is explained by a higher particle velocity in the case of HYPS. These results however are only preliminary ones because many parameters have still to be characterized systematically such as the velocity, surface temperature and velocity of the impacting particulate.

The substrate nature and temperature have also an important influence, as it will be shown in section 1.3, because they control the wettability. And at last the influence of the substrate roughness, modifying the splat spreading should also be looked at.

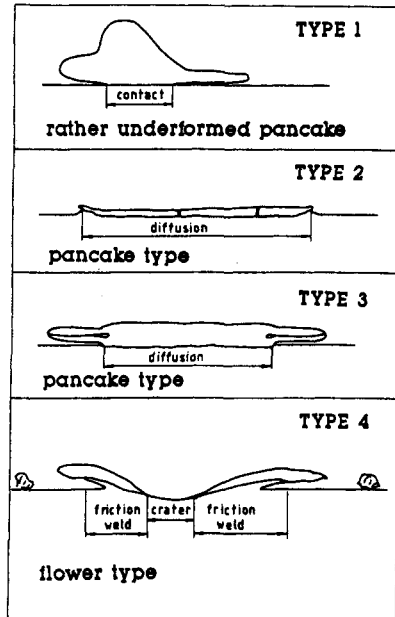


Figure 2: Main morphologies of metallic particulates sprayed on steel after Houben (ref 10)

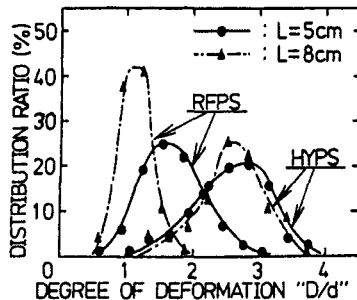


Figure 3: The effect of the distance from the torch exit (L) on the flattening degree of particles.

2. Acoustic emission monitoring

Acoustic emission (AE) monitoring has been widely used to detect critical defects in structures or to follow the behaviour of these defects under various conditions (ref 22,23,24,25).

Pacey and Stratford (ref 26) were the first to apply this method to monitor the impact of individual particulates on the substrate during plasma spraying process. One emission acoustic sensor was clamped to the rear face of the substrate. Each sprayed coating was applied for 30 seconds, during which time, AE events were detected and recorded. A typical run would capture over 10 000 events.

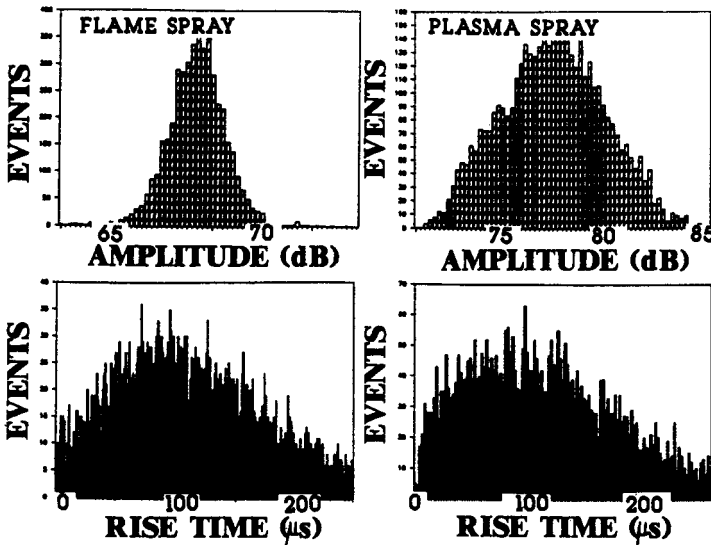


Figure 4: Amplitude and rise time distributions for flame and plasma sprayed aluminium titanate (22-45 µm)

Separate experiments were carried out to simulate the individual effects associated with different particulate conditions upon impact (liquid or solid particulate with high or low velocity).

Significant differences were found in the values of duration, amplitude, rise time and counts obtained using two different alumina-titania powders under various arc currents.

Some typical results are given in fig 4. It is worth to notice that such experiments correspond to typical times in the order of a few hundreds of microseconds while the pyrometric measurements presented in section 1.3 show that the cooling rate of the particulates is very high during 10 - 20 µs (about 1500 K), the extrapolation of the curves indicating that cooling from 2000 K to 900 - 1000 K takes about 0.1 ms. The simulation experiments suggest that short duration and rise time are associated with behaviour of hard particulates at impact but can also be produced with small degrees of particle flattening and long durations are associated with high degree of particle flattening. The physical interpretation of the rise time and duration values is still in question according to all the physical and shape changes undergone by the particulate upon first impact and then cooling.

If the differences in distributions are marked during the initial stages of spraying, they are less distinct during the later stages. This cannot be explained by simple attenuation because rise time tends to lengthen, not shorten with signal attenuation. And this difference in signals is probably due to the differing nature of the surface at the beginning and end of each run as confirmed by the experiments conducted by Moreau et al (ref 27) and presented in the next section.

3. Thermal radiation monitoring

The thermal evolution of individual particulates as they impact on a substrate may be monitored as established by Moreau et al (ref 28,29). The experimental set up shown in fig 5 was made up of a double wavelength fibre optic pyrometer focused on a typically 100 µm diameter spot on the substrate surface (in such experiments where the impacting particulate area changes with time and the emissivity varies with temperature, it is preferable to conduct two color pyrometric measurements). A second fibre optic sensor viewing the same spot at a slant angle provides coincident triggering to discriminate against in flight particulates intersecting the pyrometer field of view; the thermal history of particulates impinging on the substrate is followed with a 0.5 µs time resolution.

Infrared radiation from the pyrometer head is imaged through a beam splitter on two detectors (silicon avalanche photodiodes) filtered by two interference filters centered at 900 and 700 nm respectively.

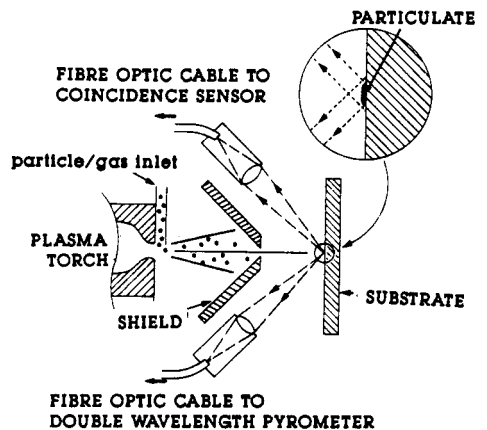


Figure 5: Experimental set up used to monitor temperature evolution of particles impacting on a substrate after ref 28.

The temperature evolution of the impacting particulate is computed after calibration from the ratio of detector output. Calibration is performed in pointing the pyrometer head to a tungsten ribbon lamp and recording the ratio signal while the ribbon temperature is determined by a two color calibrated commercial pyrometer (ref 30).

Tests with different kinds of sprayed materials (niobium, titanium carbide) and with different substrates (steel, glass, alumina) have been carried out. Thermograms corresponding to either molten or solid particulates impacts have been obtained: for the presumably solid impact, thermograms show an almost instantaneous rise to the maximum temperature followed by a gradual cooling while for liquid impact, they show a more graduate rise to the maximum temperature before starting cooling as if hotter internal liquid is unveiled as the particle flattens.

An exemple of thermal event corresponding to the impact of a niobium particulate on an alumina substrate is given in fig 6.

This thermogram presents a rapid cooling period followed by a plateau lasting approximately $1.5 \mu\text{s}$ and a second less rapid cooling period. The duration of thermal event for niobium particulates ranges from 15 to 20 μs on the glass substrate and is less than 5 μs on the steel and alumina substrates, the thermal conductivity of the glass being about one order of magnitude lower than that of steel and alumina.

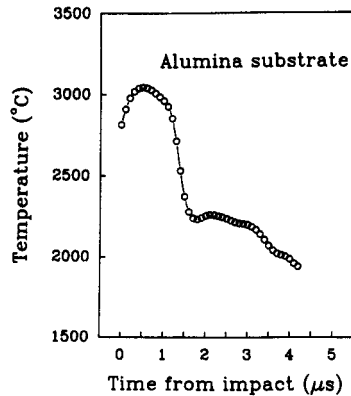


Figure 6:
Thermogram of a Niobium particulate sprayed on an alumina substrate after ref 28.

Recent experiments (ref 27) have shown that in fact the cooling time is a function of the coating thickness and thus probably of its increasing temperature. For molybdenum particulates sprayed on glass slides it varies from 15 - 20 μs when particulates impinge on the bare substrate to about 5 μs when the coating thickness exceeds 20 μm . This could be due to a better wettability improving the contact between the splat and the previously deposited layers.

Thermograms were computed from a 2D finite difference thermal propagation model (ref 28) implemented to simulate the thermal flow from the hot particulate to the substrate after impact. By comparing these experimental data with the computed ones, the transient thermal resistance at the interface of the molybdenum particulate with the substrate (glass, zirconia or copper) was estimated to be of the order of $1.2 \times 10^{-6} \text{ m}^2 \cdot \text{K} \cdot \text{W}^{-1}$ and $0.3 \times 10^{-6} \text{ m}^2 \cdot \text{K} \cdot \text{W}^{-1}$ at the Mo-Mo interface. This low thermal resistance results from the good wetting of the molybdenum surface by the molten metal.

As already emphasized in section 1.1, the particulate velocity at impact is one of the parameters governing its flattening and solidification on the substrate, therefore the experimental set up used for these experiments has been completed to measure the velocity of the impacting particulate. For this, two double wavelength optical fibre pyrometers are used: one is focussed 2 mm before the substrate and the other on the substrate as shown in fig 7. An optical sensor focussed at the same point than the first pyrometer allows to trigger signals recording when a particulate is detected simultaneously with the first pyrometer.

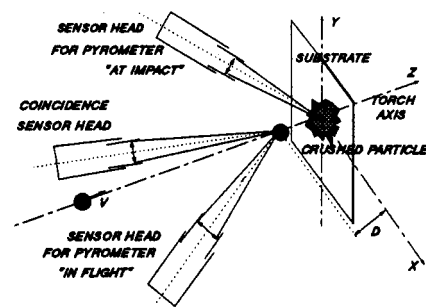


Figure 7: Schematic of the experimental set up used to follow one particulate prior and at impact on a substrate

The particulate velocity is deduced from the time of flight between the two spots; its surface temperature before impact is measured by the first pyrometer and its time-temperature profile at impact by the second pyrometer focussed on the substrate (ref 31).

Fig 8 and 9 show experimental results recorded for a tungsten particle (30 μm in diameter) sprayed on a steel substrate.

In fig 8, the first peaks correspond to in flight measurement and the second to the measurement at impact, the ratio of the two peak amplitudes for the same wavelength being an indicator of the flattening degree of the particulate. The measure of the particulate temperature before impact confirms that for thermogram shown in fig 9 the core of the particulate is hotter than its surface (the particulate has started to cool down from 60 mm of the nozzle exit). From this thermogram, the cooling rate of this particulate during the first ten microseconds is estimated to be as high as 10^8 K/s .

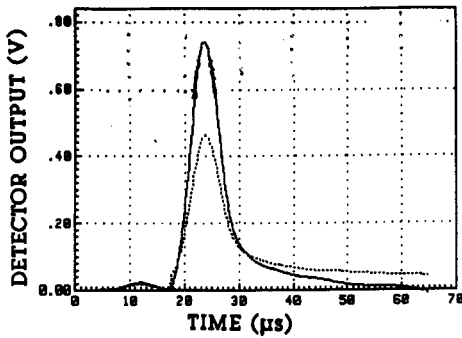


Figure 8: Typical detector outputs recorded before and after particulate impact

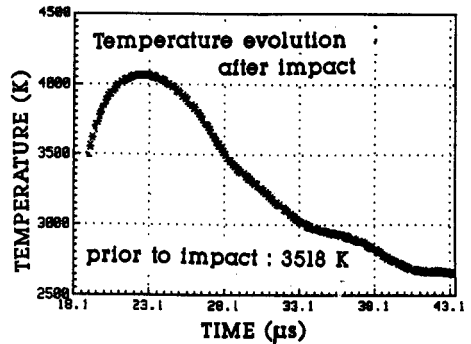


Figure 9: Time-temperature evolution after impact

PARTICULATE VAPORIZATION INTO THE PLASMA

Although the importance of particulate vaporization under thermal plasma conditions has been stressed in a number of theoretical analyses (ref 7,8) few experimental data are available about this phenomenon.

When vaporization occurs, mass transfer from the particulate surface towards the plasma gas reduces the effective heat transfer : the enthalpy directed to the surface is used to provide the latent heat of vaporization and to heat the vapor within the boundary layer. The vapor diffusion modifies the plasma gas composition and so its transport properties.

Experiments based on absorption spectroscopy using a hollow cathode lamp as an absorption source (ref 32) have shown that when alumina particulates were sprayed at 15 kW with pure argon as plasma forming gas, it was possible to measure the AlI concentration ($n_{AlI} \sim 10^{16} \text{ m}^{-3}$) 20 mm downstream the nozzle exit. For Ar-H₂ mixture (20% H₂ in vol.) with P = 17 kW due to the much better heat transfer, the AlI atoms can be detected 7 mm downstream from the nozzle exit with a maximum concentration ($\sim 3 \times 10^{19} \text{ m}^{-3}$) at 30 mm downstream. Similar results have been reported for nickel and iron powders (ref 32).

Eddy et al (ref 33,34) have studied by emission spectroscopy and flow visualization with a laser video-system, plasma jets either free of particulates or loaded with NiAl or WC/Co powders. The spectrographic measurements show that under the operating conditions investigated, W and Co are significantly vaporized and ionized resulting in a plasma mixture of the plasma forming gas (Ar-He) and W/Co. That should be taken into account when modelling thermodynamic and transport processes in the plasma particulates interactions. Nanosecond video frames of the loaded plasma jet show the powder plasma comets generated during the process.

To provide more information about particulate vaporization, it is necessary to study these comets. A technique based on emission spectroscopy allowing to investigate the vapor cloud surrounding a single particulate is given in (ref 35). The temperature within this "diffusion zone" is determined by the intensity ratio of the vapor lines simultaneously measured. Its radius is deduced from the measurement of particulate velocity by laser doppler anemometry and the vapour concentration is calculated from the absolute line intensity profile, once temperature is known.

The experimental set up is shown in fig 10. The image of the measuring volume is made on the entrance slit of a monochromator (JY HR 1000) with a magnification of two. The light pulses received by the monochromator when a particulate is passing through the observation zone are simultaneously detected by two optical fibres (200 µm in diameter). The focal field in the plasma flow corresponds approximatively to a cylinder whose diameter is equal to 100 µm and length to 15 mm. A detector set on an axis perpendicular to the line of sight enables to restrict the length of this cylinder to 1 mm. A synchronisation unit ensures the selection of the studied signals which are processed by an oscilloscope which digitalizes the pulses with a sampling rate of 100 MHz.

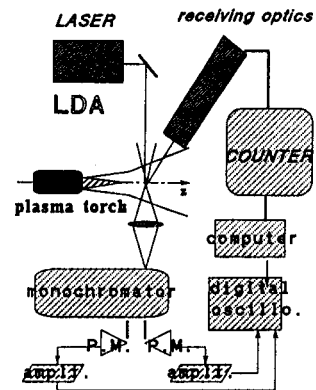


Figure 10: Experimental set up used for investigation of particulate vaporization

The data are processed using a specifically developed algorithm whose main operations are the following:

- regrouping of points for each signal (each one being made up of 5000 points)
- locating of symmetry axis
- smoothing of the averaged signal
- Abel's inversion (at the present time, only symmetric signals are processed, the selection being carried out by form recognition).

These operations are carried out for the two signals simultaneously recorded and the temperature is determined from the ratio of the emission coefficients of the two lines.

The measurement of the particulate velocity by laser doppler anemometry enables to change the temporal evolution of the temperature into a spatial one, assuming that the velocity of a particulate and its vapor cloud are identical. This assumption is verified for distances higher than 45 mm from the powder injection port, whereas at the beginning of particulate trajectory, the plasma velocity is by far much higher than that of the particulates.

Assuming a Boltzmann distribution, the metallic atoms concentration in the vapor cloud is calculated from the line intensity profiles once temperature evolution and cloud radius are known. To obtain absolute values for the integral intensities of spectral lines, the radiation of the investigate source is compared to that of a tungsten ribbon lamp with quartz window. This comparison is made under strictly identical conditions using the same optical elements, equal apertures...

Results obtained with WC/Co particulates sprayed in an Ar-H₂ plasma jet are given in fig 11 and 12, each curve corresponding to the average calculated on 20 events (these data are issued from a joint study between the University of Limoges and the Idaho National Engineering Laboratory).

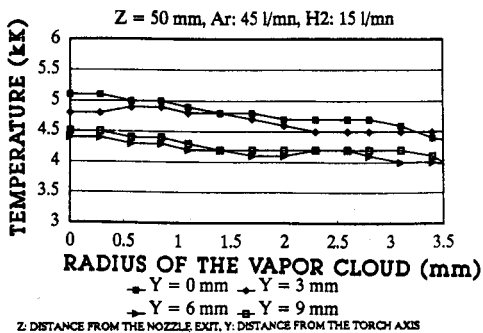


Figure 11:

Temperature distribution within the comets (50 mm from the nozzle exit) for different distances Y from the plasma jet centerline

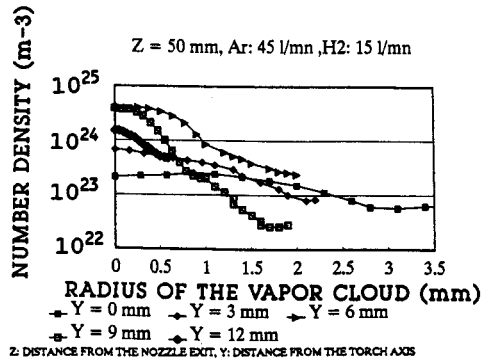


Figure 12:

Co concentration distribution within the comets (50 mm from the nozzle exit) for different distances Y from the plasma jet centerline

The radius of the cloud are estimated to be of the order of 1 - 1.5 mm. These values correspond to 10% of the maximum value of the concentration profiles. The temperature is nearly constant within the vapor cloud and equal to the temperature of the plasma jet at the same distances from the nozzle exit. Very high values for the Co atom concentration ($\sim 10^{24} \text{ m}^{-3}$) can be observed near the particulate wall. The evolution of the comets radii at different radial locations in a plasma jet cross section may be explained by the different trajectories followed by the investigated particulates. Studies have yet to be made to determine the influence of this vapor cloud on the particulate flattening.

CONCLUSION

Many statistical measurements of the velocity, surface temperature, diameter of particulates in flight in d.c. spraying plasma jets have confirmed the wide variety of treatments undergone. This is due to the trajectories dispersion induced by the size and injection velocity distribution of the particulates. It explains the very different morphologies of the splats collected at different distances downstream of the nozzle exit. These widely different shapes and morphologies of the resulting lamellae are related to the

particulates velocity, diameter, temperature and temperature gradient upon impact. They influence deeply the contacts between the lamellae as shown for example by Houben (ref 10) and Mc Pherson (ref 13), contacts controlling the resulting thermo-mechanical properties of the coatings. That is why it is mandatory to understand better the phenomena involved during the impact, the flattening and the cooling of one particulate which velocity, diameter and surface temperature are known. Recent works have allowed successively to determine: these parameters for one particulate in flight (ref 36), the surface temperature evolution of one particulate during its flattening and cooling down to 2000 K (ref 27,28), the same plus its velocity and surface temperature prior to impact (ref 5). These works have underlined very interesting points such as flattening in less than 1 μ s, fast cooling (1500 K drop) in less than 20 μ s, followed by a much slower cooling rate. Very preliminary results show also the influence of the substrate temperature probably due to wettability modification. Moreover measurements in flight show that the particulates are surrounded by big vapor clouds (5 - 20 times their diameter) influencing also probably their flattening. Thus the tools to study systematically the particulates flattening and cooling are progressively developed. Once these phenomena will be understood, they will provide a set of rules describing the physics of how the splats interact with each other to build a coating which generation could be modelled by statistical analysis.

REFERENCES

1. J.H. Zaat, Ann. Rev. Mater. Sci., 13,9(1983).
2. Thermal Spraying, (ed.) American Welding Society., Miami, Fl.,USA(1985).
3. E. Pfender, Pure and Applied Chemistry., 57,9,1179(1985).
5. P. Fauchais, J.F. Coudert, A and M. Vardelle, Thermal Spray: Advances in coatings technology, edited by David L. Houck, ASM International, Metals Park, Ohio 44073,11(1988).
6. F. Akao, K. Akari, S. Mori, and A. Moriyama, Trans. Iron Steel Inst. Jpn 20,737(1980).
7. Xi Chen, Y.P. Chyow, Y.C. Lee, and E. Pfender, Plasma Chem. Plasma Process.,5,119(1985).
8. P. Proulx, J. Mostaghimi, M. Boulos, Colloque de Physique C5, 51, 253(1990).
9. M. Vardelle, C. Trassy, A. Vardelle, P. Fauchais, Plasma Chem. Plasma Process., 11, 185(1991).
10. J.M. Houben., in F.N. Longo (ed.), Proceedings of the Second National Conference on Thermal Spray, ASM., 1(1984).
11. D. Apelian, M. Paliwal, R.W. Smith, W.f. Schilling, International Metals Reviews., 28, 5,271(1983).
12. J. Madejski, Int. J. Heat Mass Transfer., 19, 1009(1976).
13. R. Mc Pherson, Journal of Materials Science., 15, 3141(1980).
14. H. Hamatani, T. Okada, T. Yoshida, ISPC9 Pugnochuso Italie., 1,1527(1989).
15. L. Pawlowski, D. Lombard, P. Fauchais, J. Vac. Sc. Technol., A3,6,2494(1985).
16. E. Carrity, Dan Wei, D. Apelian, Modeling of Casting and Welding Process, edited by A.F. Giamei and G.J. Abraschian, Metals & Materials Society., (1988).
17. R. Mc Pherson, Thin Solid Films.,83, 297(1981).
18. Y.A. Kharlamov, M.S. Hassan, R.N. Aderson, Thin Solid Films, 63, 111(1979).
19. S.J. Yankee, B.J. Pietka, Proceedings of the National Thermal Spray Conference., 4, Pittsburg, (1991) to be published by ASM.
20. V.V. Kudinov, P. Yu. Pekshev, V.A. Safivllin, High. Temp. Dust Laden Jets, Solonenko and Fedorchenko (eds.), 381(1989).
21. M. Boulos, Proc. 2st Plasma Technik Symp., (Luzern, Switzerland), 49(1991).
22. D. Almond, N. Moghisi, and H. Reiter, Thin Solid Films., 108, 439(1983).
23. P. Ostojic, and R. Mc Pherson, Thin Solid Films., 136, 215(1986).
24. S. Safai, H. Herman, and K. Ono, 9th International Thermal Spraying Conference., The Hague, 129(1980).
25. H.D. Steffens, and H.A. Crostack, 9th International Thermal Spraying Conference, The Hague, 120(1980).
26. R.A. Pacey, V. Stratford, Proc. 1st Plasma-Technik Symp. (Luzern, Switzerland), 485(1988).
27. C. Moreau, M. Lamontagne, P. Cielo, NTSC 91, Session Processing Science 2, (Pittsburgh), (1991) to be published by ASM.
28. C. Moreau, P. Cielo, M. Lamontagne, S. Dallaire, M. Vardelle, Meas. Sci. Technol. 1,807(1990).
29. C. Moreau, P. Cielo, M. Lamontagne, S. Dallaire, M. Vardelle, in Thermal Spray Research and Applications 19(1990) ed. T.F. Bernecki ASM International.
30. J. Mishin, M. Vardelle, J. Lesinski, P. Fauchais, J. Phys. E: Sci. Instrum., 20,620(1987).
31. M. Vardelle, S. Fontassi, C. Moreau, P. Fauchais, submitted to J. Phys. E: Sci. Instrum.
32. M. Vardelle, A. Vardelle, P. Fauchais, C. Trassy, Intern. Symp. on Plasma Chemistry 8, K. Akashi (ed.), (University of Tokyo), 1,404(1987).
33. B.A. Detering, J.R. Knibloe, T.L. Eddy, Proceedings of the Third National Thermal Spray Conference, Long Beach (USA), 27(1990).
34. T.L. Eddy, B.A. Detering, G.C. Wilson, Proceedings of the Third National Thermal Spray Conference, Long Beach (USA), 33(1990).
35. M. Vardelle, C. Trassy, A. Vardelle, P. Fauchais, Plasma Chemistry and Plasma Processing, 11,2,185(1991).
36. T. Sakuta, and M.I. Boulos, ISPC-8, Tokyo, August 31. Sept.4, 1, 371(1987).